Magnetoresistance of graphene-based spin valves

L. Brey[1] and H. A. Fertig[2,3]
[1]*Instituto de Ciencia de Materiales de Madrid (CSIC), Cantoblanco, 28049 Madrid, Spain*
[2]*Department of Physics, Indiana University, Bloomington, Indiana 47405, USA*
[3]*Department of Physics, Technion, Haifa 32000, Israel*
(Received 10 October 2007; published 26 November 2007)

We study the magnetoresistance of spin-valve devices using graphene as a nonmagnetic material to connect ferromagnetic leads. As a preliminary step, we first study the conductivity of a graphene strip connected to metallic contacts for a variety of lead parameters and demonstrate that the resulting conductivity is rather insensitive to them. We then compute the conductivity of the spin-valve device in the parallel and antiparallel spin polarization configurations and find that it depends only weakly on the relative spin orientations of the leads, so that the magnetoresistance (MR) of the system is very small. The smallness of MR is a consequence of the near independence of the graphene conductivity from the electronic details of the leads. Our results indicate that, although graphene has properties that make it attractive for spintronic devices, the performance of a graphene-based spin-valve is likely to be poor.

DOI: 10.1103/PhysRevB.76.205435 PACS number(s): 73.20.−r, 73.22.−f, 72.25.−b

I. INTRODUCTION

Recently, it has become possible to isolate an individual graphene layer,[1] a two dimensional crystal of carbon atoms packed in a honeycomb lattice. When deposited on top of a doped dielectric substrate, the density of carriers moving in the graphene sheet can be modified by applying a gate voltage.[2,3] At low energies, carriers moving in a graphene sheet obey the Dirac equation, so that graphene offers the interesting possibility of studying the properties of Dirac fermions. Apart from the interesting fundamental physics of this new system, graphene is attracting attention as a promising new material for microelectronic applications.

The conductivity of graphene tends to a minimum value when the density of extra carriers tends to zero.[2–4] Theories predict a universal value, $\sigma_u = 4e^2/\pi h$, for the conductivity of a homogeneous and impurity-free undoped graphene sheet.[5–9] However, experimental values of the minimum value of the conductivity in graphene sheets is between five and ten times larger than the theoretical prediction. This discrepancy may occur because in neutral graphene, the system breaks up into electron and hole puddles,[10] so that transport could occur through the resulting holelike and electronlike regions.[11] The charge puddles may appear in order to screen impurities which are invariably present,[12] or may be induced by ripples in the graphene sheets.[13–17]

In the ballistic regime, theoretical work[18–21] has shown that the conductivity of an intrinsic graphene sheet of width W and length L takes the universal value in the $W/L \to \infty$ limit. Such a ballistic approximation is valid when the mean free path of the carriers is larger than the sample dimensions. This was the case, for example, for devices used in Ref. 22, which confirmed that the conductivity of wide and short graphene ribbons tends to the universal value of $4e^2/\pi h$.

Graphene exhibits room temperature mobilities above 10^5 cm^2/V s^2, implying that electrons in graphene sheets can move very long distances without scattering. For short range scatters, the mean free path can be as large as 1000 nm.[23] From these results, we expect the ballistic approximation to be appropriate in describing transport in graphene nanoribbons.[24,25] In addition, the small spin-orbit coupling of carbon atoms[26] results in a long spin lifetime for carriers in graphene sheets. This makes graphene a very good candidate for microelectronic and spintronic applications.

In developing new spintronic devices, it is very important to find nonmagnetic materials where a spin-polarized current can be injected and flow without becoming depolarized. The most popular existing spintronic devices are spin valves. These devices use the fact[27] that the electrical resistance of a nonmagnetic material connected to spin-polarized source and drain leads depends strongly on their relative spin orientation. Spin valves are promising candidates for systems that may transform spin information into electrical signals. These devices perform best when the spin relaxation time of the nonmagnetic material is long, making graphene a good candidate for this component of a spin valve. Moreover, the combination of weak spin-orbit coupling and low hyperfine interaction of the electron spin with the carbon nucleus makes graphene a good candidate for other spintronic applications such as spin qubits,[28] three-terminal devices,[29,30] and spin filters.[31]

Recently, several groups have performed nonlocal four-probe measurements[32–34] of graphene, connected to ferromagnetic electrodes, and have demonstrated the presence of spin currents between injector and detector. These experiments provide proof, in principle, of the possibility of injecting a spin current into graphene, with a spin relaxation length larger than 2 μm at room temperature.[32] Moreover, a magnetoresistance of several hundred ohms was observed in a spin valve where graphene is contacted by two ferromagnetic electrodes.[35] These experiments clearly demonstrate the potential for graphene in spintronic devices.

In this work, we study the magnetoresistance of a graphene-based spin valve. This is a three component device, with a first ferromagnetic lead used as a spin polarizer, a nonmagnetic spacer—graphene in our case—and a second ferromagnetic lead used as analyzer. We consider two kinds of electrodes (see Fig. 1): (a) a single orbital band metal where the center of the minority spin band is shifted with

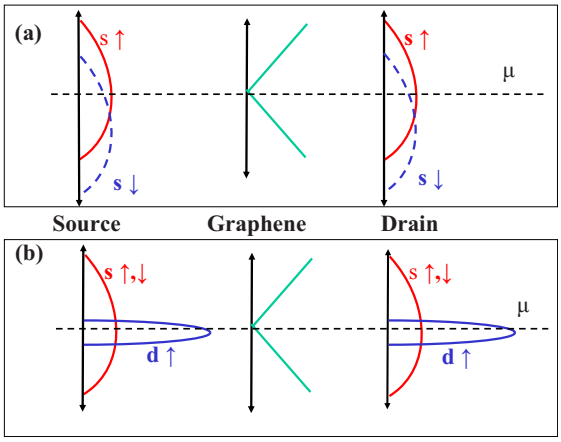

FIG. 1. (Color online) Schematic representation of the spin valves studied in this work. We plot the density of states of the central graphene region and of the ferromagnetic source and drain leads. In (a), the leads are single orbital band metals where the center of the minority spin band is shifted with respect to the majority spin band. (b) corresponds to the case of a ferromagnetic transition metal with a spin-polarized narrow d band and a paramagnetic wide s band. The horizontal dashed line indicates the chemical potential μ. In this schematic picture, $\mu=0$. In both cases, the spin polarizations of the leads are illustrated in the parallel configuration. For the antiparallel configuration, the spin labels of each band in the drain lead should be reversed.

respect to the majority spin band in such a way that the material is ferromagnetic (this is a simplified version of a dilute magnetic semiconductor) and (b) a ferromagnetic transition metal (e.g., cobalt) with a spin-polarized narrow d band and a wide paramagnetic s band at the Fermi energy.

We assume the carrier mean free path in graphene is longer than the dimension of the graphene part of the device, so that the transport properties can be calculated in the *ballistic approximation*. In addition, since the spin-orbit coupling in graphene is very small, it is appropriate to assume that the spin diffusion length is sufficiently long that the carriers do not undergo spin flips while traversing the graphene. Therefore, we model the transport in terms of two independent spin channels.[36] In this work, we will call this the independent current model.

This paper is organized as follows. In Sec. II, we describe the Green's function formalism for computing the conductance of a ballistic system[37] and show how this leads to a *conductivity* for undoped graphene. In Sec. III, we then apply the formalism to compute the magnetoresistance of a wide piece of graphene contacted by two single orbital band ferromagnetic leads. In Sec. IV, we discuss the case of transition metal leads, modeled as conductors with two orbital bands, one narrow and one wide. We then compute the magnetoresistance of this system. Finally, we summarize our results in Sec. V.

II. CONDUCTANCE AND CONDUCTIVITY OF A GRAPHENE STRIP

We begin by first calculating the conductance of a graphene strip connected to single orbital metallic leads [see Fig. 1(a)] for an arbitrary alignment of the lead band bottoms and the Dirac points of the graphene system.

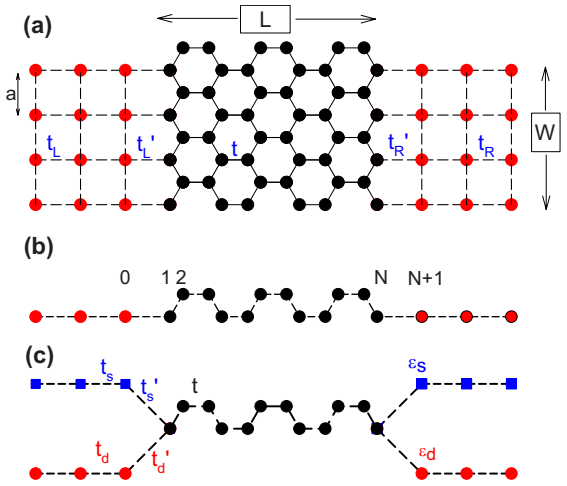

FIG. 2. (Color online) (a) Structure of the spin valve studied in this work. A graphene sample is connected to metallic leads which are modeled as commensurably matched square lattices. (b) Unit cell that is periodically repeated in the y direction in the case of a graphene strip connected to single orbital metallic leads. (c) Unit cell in the case of a graphene strip connected to ferromagnetic transition metal leads. Square (blue) points describe the s atoms, and circle (red) points represent d atoms.

A. System description

We consider a strip of graphene as illustrated in Fig. 2(a), with lattice parameter a, attached to metallic leads which are each modeled by a commensurably matched square lattice with the same lattice parameter.[20,21] The graphene strip has length L in the x direction and is infinitely wide in the y direction, i.e., $W\to\infty$. With this geometry, we can define a unit cell, infinitely long in the $\hat{x}$ direction, that is periodically repeated in the y direction [Fig. 2(b)]. In order to match the graphene sample to the square lattice leads, the number of carbon atoms in the unit cell, N, should be a multiple of 4, so that the length of the graphene sample is $L=N/4\sqrt{3}a$.

B. Hamiltonian

The electronic properties of the graphene are described by a tight-binding Hamiltonian with nearest neighbor hopping t and zero on-site energy. The left (L) and right (R) metallic leads are also described by tight-binding Hamiltonians, with nearest neighbor hopping amplitudes t_L and t_R and on-site energies ε_L and ε_R, respectively. The graphene sample is connected to the left and right leads with hopping amplitudes t_L' and t_R', respectively.

Because of the discrete translational invariance in the y direction, we can label the eigenvalues and eigenvectors of the Hamiltonian by a momentum k_y in the y direction that takes values in the range $-\pi/a<k_y<\pi/a$. The limit $W\to\infty$ is obtained by treating this as a continuous variable. In order to simplify notation, in the rest of the paper, the wave

vector k_y will be given in units of $1/a$. With this, the electronic properties of the two dimensional problem are reduced to a set of k_y-dependent one dimensional Hamiltonians with on-site energies (see Fig. 1),

$$\epsilon_i = \begin{cases} \epsilon_L + 2t_L \cos k_y & \text{if } i \leqslant 0 \\ \epsilon_R + 2t_R \cos k_y & \text{if } i \geqslant N+1 \\ 0 & \text{if } 1 < i < N, \end{cases} \tag{1}$$

and hopping amplitudes t_i between sites i and $i+1$,

$$t_i = \begin{cases} t_L & \text{if } i < 0 \\ t'_L & \text{if } i = 0 \\ t + te^{ik_y} & \text{if } i = 1,5,9,\ldots, \quad \text{and } 0 < i < N-1 \\ t & \text{if } i = 2,6,10,\ldots, \quad \text{and } 0 < i < N-1 \\ t + te^{-ik_y} & \text{if } i = 3,7,11,\ldots, \quad \text{and } 0 < i < N-1 \\ t & \text{if } i = 4,8,12,\ldots, \quad \text{and } 0 < i < N-1 \\ t'_R & \text{if } i = N \\ t_R & \text{if } i > N. \end{cases} \tag{2}$$

C. Conductance

The conductance per spin channel of the system takes the form

$$G(\mu) = \sum_{k_y} g^{1D}(\mu, 2t_L \cos k_y + \epsilon_L), \tag{3}$$

where μ is the chemical potential and $g^{1D}(E, \epsilon_0)$ is the conductance of the one dimensional chain with an on-site energy ϵ_0 in the left electrode, evaluated for Fermi energy E. (Note that g^{1D} implicitly depends on the on-site energy in the right lead as well.) The one dimensional conductance is given by[37]

$$g^{1D}(\mu, 2t_L \cos k_y + \epsilon_L) = \frac{e^2}{h}\Gamma_1(\mu)\Gamma_N(\mu)|G_{1,N}(\mu)|^2, \tag{4}$$

where $\Gamma_1(E) = i(\Sigma_1 - \Sigma_1^+)$ and $\Gamma_N(E) = i(\Sigma_N - \Sigma_N^+)$ are the injection ratios, and Σ_1 and Σ_N are the self-energy terms due to the leads attached at sites 1 and N, respectively,[37]

$$\Sigma_{1(N)}(\mu) = t'_{L(R)} e^{-ik_{L(R)}}, \tag{5}$$

with

$$k_{L(R)} = \arccos\left(\frac{\mu - \epsilon_{L(R)} - 2t_{L(R)} \cos k_y}{2t_{L(R)}}\right). \tag{6}$$

In Eq. (4), $G_{1,N}(\mu)$ is the effective Green's function for the system, evaluated in the graphene region:

$$G_{1,N}(\mu) = \frac{1}{\mu - H_c - \Sigma_1(\mu) - \Sigma_N(\mu)}. \tag{7}$$

Here, H_c is the one dimensional k_y-dependent Hamiltonian of the graphene sample described by the on-site energies and hopping amplitudes given in Eqs. (1) and (2).

Finally, the conductivity of the device is related to the conductance through geometrical factors,

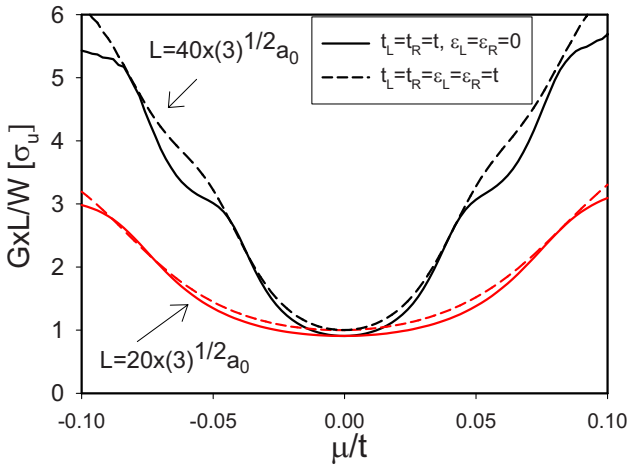

FIG. 3. (Color online) Conductivity in units of $\sigma_u = 4/\pi(e^2/h)$, as a function of the chemical potential for two different graphene sample lengths and two sets of parameters describing the lead band structures. The conductivity shows a minimum at the Dirac point, which is independent of the sample length.

$$\sigma(\mu) = \frac{L}{W} G(\mu). \tag{8}$$

In two dimensions, conductivity and conductance have the same units. However, the former is only useful in systems where its value is sample-size independent for large L and W. Usually, this is only the case for diffusive systems. Remarkably, as has been pointed out previously[18,20] and as we demonstrate explicitly below, for undoped graphene, it is true in the *ballistic* limit, provided we take $W \to \infty$ before taking $L \to \infty$.

In Fig. 3, we plot $G(\mu) \times L/W$ in units of the universal conductivity for two sets of parameters for the leads, in the limit of large W, and for two different values of L. One may observe from these results that except for $\mu = 0$, the conductance is essentially independent of L. Interestingly, the conductance is relatively insensitive to the details of the metallic leads; its overall shape is mostly determined by the graphene density of states. In particular, the roughly linear rise as μ moves away from zero may be understood as reflecting the linear density of states of graphene. The shoulders in the conductance riding on this linear background correspond to Fabry-Pérot resonances due to the finite length of the graphene sample.[38] The amplitude of these resonances is determined by the parameters of the leads.

In the case of intrinsic (i.e., undoped) graphene—$\mu = 0$—the electronic transport behaves as if it is diffusive, and the conductivity is well defined. For $t_L = t_R = t'_L = t'_R = t$ and $\varepsilon_L = \varepsilon_R = 0$, we obtain $\sigma = \sqrt{3}/2(e^2/h)$, in agreement with Ref. 20. This value changes when the centers of the energy bands in the leads change. The conductivity reaches the universal value, $\sigma_u = 4/\pi(e^2/h)$, when $\varepsilon_L = t_L$ and $\varepsilon_R = t_R$.[18,20]

The $\mu = 0$ case may be worked essentially analytically, because transport is dominated by values of k_y in the vicinity of the Dirac points $\left(0, \pm\frac{4\pi}{3a}\right)$. In this case and for large values of L, it is possible to explicitly evaluate the transmission

probability associated with H_C for each valley and spin channel using a transfer matrix method, with the result

$$T_{k_y}(\mu=0)=\frac{4\xi t^2 \sin k_L \sin k_R}{\xi^2 e^{2Lk_y}+t^4 e^{-2Lk_y}-2t^2\xi\cos(k_L+k_R)}. \quad (9)$$

In this expression, the parameter $\xi=(t_L'^2 t_R'^2)/(t_L t_R)$ contains the information about the coupling to the leads, the wave vector k_y is defined with respect the Dirac point, and k_L and k_R are defined in Eq. (6). For μ at the Dirac points, there are *no* individual propagating modes in the graphene sample connecting the metallic leads at any finite value of k_y, and the transmission probability vanishes in the limit $L\to\infty$.

By integrating the transmission amplitude [Eq. (9)] over k_y, we obtain the $\mu=0$ conductance,

$$G=\frac{e^2}{h}\frac{2g_s g_v}{\pi}\frac{W}{L}\frac{\sin k_L \sin k_R}{\sin(k_L+k_R)}\arctan\left(\frac{\sin(k_L+k_R)}{1-\cos(k_L+k_R)}\right), \quad (10)$$

where $g_s=2$ and $g_v=2$ are the spin and valley degeneracies, respectively. Remarkably, although all the modes are evanescent, the total conductance falls off only as $1/L$, so that the electrical transport is Ohmic. This behavior arises because the effective length scales of the evanescent modes are each $1/k_y$, which is arbitrarily large as $k_y\to 0$, resulting in the relatively weak $1/L$ behavior for G. (Alternatively, the finite value of the transmission probability near the Dirac points may be understood in terms of virtual electron-hole pair excitations near zero energy in the graphene region.[18]) By contrast, for systems in which μ may lie in a gap, the effective length scale for wave functions is bounded by a distance that is determined by the difference between μ and the bottom of the conduction band for the "conducting" region. Because of this maximum length scale, G falls off exponentially with L, and the conductivity, as well as the conductance, vanishes as $L\to\infty$. Thus, clean graphene is rather unique in displaying Ohmic behavior.

Another remarkable feature of this result is that the conductivity does not depend on the couplings t_L' and t_R' of the metallic leads with the graphene sample. This result is only possible in the limit $W\to\infty$, since for any finite value of W, the two leads become fully disconnected if either of these parameters vanishes, and the conductance must vanish. However, in the infinite width limit where the momentum sum becomes an integral, the parameter ξ through which t_L' and t_R' enter scales out, and the final result is independent of these parameters.

Finally, it is interesting to examine the dependence of the conductivity on the parameters specifying the leads. From the definition of k_L and k_R, one can see that the conductance depends on the lead parameters only through the combinations $(\epsilon_R-t_R)/t_R$ and $(\epsilon_L-t_L)/t_L$. In Fig. 4, we plot the conductivity, $\sigma=G\times L/W$, as a function of these combinations. The conductivity is maximized when $t_L=\varepsilon_L$ and $t_R=\varepsilon_R$, independent of the values of t_L and t_R. Because of conservation of energy and of the transverse momentum k_y, transport through the graphene ribbon when $\mu=0$ is possible only when the band centers of the left and right leads are in the intervals $2t_L<|\epsilon_L-t_L|$ and $2t_L<|\epsilon_L-t_L|$, respectively. In Ref. 20, Schomerus suggests that the conductivity of a graphene sample connected to metallic leads is maximum when the self-energies of electrons in the leads have the same value as the self-energy of bulk graphene with energy at the Dirac point ($-it$). In the square lattice, the self-energies of the incoming and outcoming electrons, evaluated at the momentum and energy of the Dirac point, are $-t_L e^{ik_L}$ and $-t_R e^{ik_R}$, respectively. Our results indicate that when the *real* part of the lead self-energies $\Sigma_1(\mu=0)$ and $\Sigma_N(\mu=0)$ [Eq. (5)] vanishes, the conductivity of the system is maximized. This condition is similar to but less restrictive than that proposed in Ref. 20 and is related to the independence of the graphene universal conductivity from the hopping amplitude t.

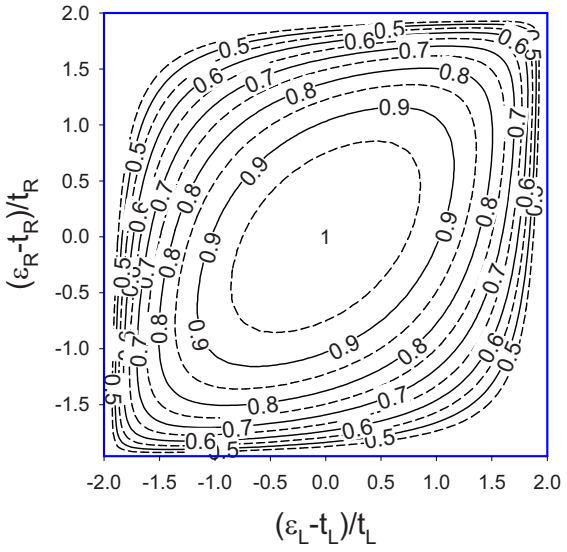

FIG. 4. (Color online) Conductivity evaluated at the Dirac point, $\mu=0$, in units of $\sigma_u=4/\pi(e^2/h)$, as a function of the source and drain lead parameters.

III. MAGNETORESISTANCE: SINGLE BAND LEADS

In this section, we apply the results derived above to find the magnetoresistance of a spin-valve device with a graphene strip at its center. In a single band ferromagnetic metal, the centers of the spin up ($\varepsilon_{0,\uparrow}$) and spin down ($\varepsilon_{0,\downarrow}$) bands are shifted, as illustrated in Fig. 1(a). This implies a relative spin polarization P of the carriers at the Fermi energy μ given by

$$P=\frac{t_\downarrow \mathbb{K}\left(\sqrt{1-\left(\frac{\mu-\varepsilon_{0,\uparrow}}{2t_\uparrow}\right)^2}\right)-t_\uparrow \mathbb{K}\left(\sqrt{1-\left(\frac{\mu-\varepsilon_{0,\downarrow}}{2t_\downarrow}\right)^2}\right)}{t_\downarrow \mathbb{K}\left(\sqrt{1-\left(\frac{\mu-\varepsilon_{0,\uparrow}}{2t_\uparrow}\right)^2}\right)+t_\uparrow \mathbb{K}\left(\sqrt{1-\left(\frac{\mu-\varepsilon_{0,\downarrow}}{2t_\downarrow}\right)^2}\right)}, \quad (11)$$

where $\mathbb{K}$ is the complete elliptic integral of the first kind, and $t_\uparrow$ and $t_\downarrow$ are the hopping matrix elements in the spin up and spin down channels, respectively. Equation (11) is obtained directly from the density of states at energy E of a square lattice with hopping parameter t and on-site energy ε_0, which is given by[39]

$$\rho(E) = \frac{1}{\pi^2 t}\Theta(2t - |E - \varepsilon_0|)\mathbb{K}\left(\sqrt{1 - \frac{(E-\varepsilon_0)^2}{4t^2}}\right). \quad (12)$$

The transport through a nonmagnetic material connected to ferromagnetic metals is expected to depend strongly on the magnitude and relative orientation of the polarizations of the leads. The magnetoresistance (MR) is defined as the relative change of the resistance when the relative spin orientation of the leads changes from parallel, R_{para}, to antiparallel, R_{anti}. In the ballistic approximation, the MR can be written as

$$\mathrm{MR} = \frac{R_{anti} - R_{para}}{R_{anti}} = \frac{G_{para} - G_{anti}}{G_{para}}, \quad (13)$$

where G_{para} and G_{anti} are the conductances of the system when the relative polarization of the leads is parallel or antiparallel, respectively.

When the nonmagnetic material is an insulator, the transport is through tunneling processes. Assuming that tunneling transport is proportional to the density of states at the Fermi energy, Julliere[40] proposed the following expression for the tunneling magnetoresistance (TMR):

$$\mathrm{TMR} = \frac{2P^2}{1 + P^2}. \quad (14)$$

Julliere's expression works rather well for TMR even for materials with complicated band structures.[41] It predicts correctly that the MR increases as the leads become more spin polarized. In this section, we study the MR when the nonmagnetic material is graphene and analyze the results as a function of the spin polarization of the leads.

In the independent current model, and using the ballistic approximation, G_{para} is the sum of the spin up conductance, Eq. (3) evaluated with $\varepsilon_L = \varepsilon_R = \varepsilon_{0,\uparrow}$, and the spin down conductance, Eq. (3) evaluated with $\varepsilon_L = \varepsilon_R = \varepsilon_{0,\downarrow}$. In the case of antiparallel spin polarization of the leads, G_{anti} is the sum of Eq. (3) evaluated with $\varepsilon_L = \varepsilon_{0,\uparrow}$ and $\varepsilon_R = \varepsilon_{0,\downarrow}$ and Eq. (3) evaluated with $\varepsilon_L = \varepsilon_{0,\downarrow}$ and $\varepsilon_R = \varepsilon_{0,\uparrow}$.

In Fig. 5, we plot the MR of a graphene-based spin valve as function of the positions of the center of the spin up and spin down bands. We consider only intrinsic graphene ($\mu = 0$), and the hopping parameter in the metallic leads is taken equal to that in the graphene part of the device, $t_L = t_R = t$. The graphene slab is extrapolated to infinite length, although for L larger than about $20a$, the results are essentially the same.

We observe that, in general, the magnetoresistance is small. Only when the parameters are such that one of the spin bands is close to or in the forbidden transport region, $2t < |\varepsilon_{0\sigma} - t|$, does one find MR to be a significant fraction of 1, and when one of the spin bands is in the forbidden region, then MR, of course, reaches its maximum possible value. Thus, in order to get a moderate value of the magnetoresistance, a large shift between the center of the spin bands in the leads is needed.

The reason for the smallness of MR is the weak dependence of the graphene conductance on the parameters of the leads (see Figs. 3 and 4). This weak dependence, particularly on the density of states of the incoming electrons, also implies an absence of any strong correlation between the spin

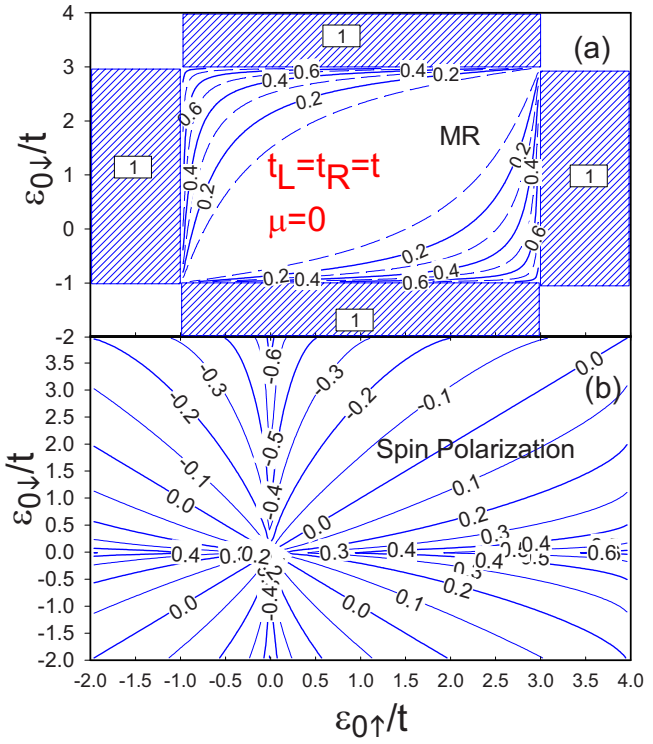

FIG. 5. (Color online) (a) Magnetoresistance (MR) and (b) spin polarization at the Fermi energy, as a function of the centers of the spin bands, of a graphene spin valve. The device consists of a long graphene slab separating single band ferromagnetic metals, Fig. 1(a). The chemical potential $\mu = 0$, and $t_L = t_R = t$.

polarization of the incoming electrons [Fig. 5(b)] and the magnetoresistance [Fig. 5(a)]. By comparing the values of the polarization and the magnetoresistance, we observe that the Julliere's expression, Eq. (14), fails to describe the magnetotransport properties of graphene-based transistors.

Note also that because the conductivity of undoped graphene is independent of the tunneling amplitude connecting the graphene with the ferromagnetic metallic leads [Eq. (10)], the magnetoresistance is also unaffected by changes in the quality of the connection between the leads and the graphene. This indicates that the smallness of the magnetoresistance in graphene-based devices is not due to a conductivity mismatch, as is the case in metal-semiconductor diffusive junctions,[42] but rather is due to the *universal* minimum conductivity of graphene, so that a "shutoff" of one spin channel is difficult to achieve.

In Fig. 6, we have plotted the spin polarization as a function of position in our graphene-based spin valve. For this calculation, the lead parameters were chosen so that the spin polarization in the leads was approximately 60%. Several points are worth noting. (1) The spin polarization decays to a zero over a length scale of about 20 lattice parameters. (2) The spin polarization is oriented in *opposite directions* for electrons on different sublattices. (3) The total induced spin in the graphene region vanishes. These effects are explained by the strong tendency for local magnetic moments in graphene to orient ferromagnetically for sites on the same sublattice and antiferromagnetically for sites on different

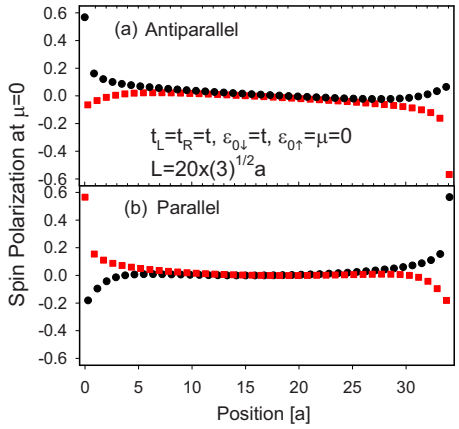

FIG. 6. (Color online) Spin polarization, evaluated at the Fermi energy, as a function of the position along the graphene slab of a graphene-based spin valve. We plot the $\mu=0$ case. (a) and (b) correspond to antiparallel and parallel configurations, respectively. Square and dot symbols indicate the spin polarization on the two types of lattice sites of the honeycomb lattice. The band structure parameters are indicated in the inset of the figure. The length of the graphene slab is $L=20\sqrt{3}a$.

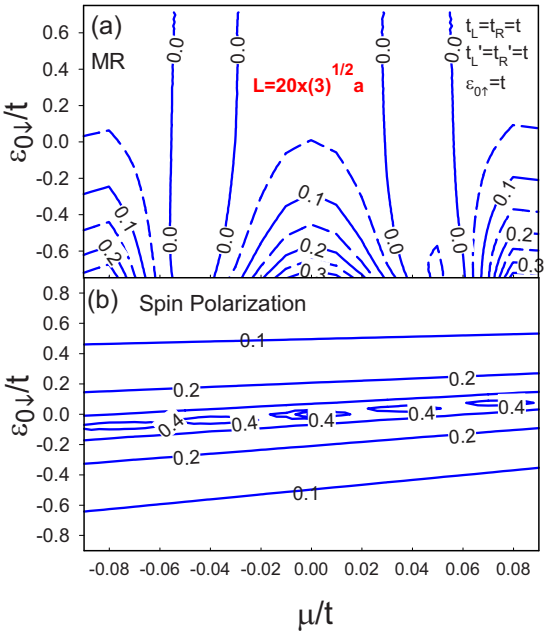

FIG. 7. (Color online) (a) Magnetoresistance (MR) and (b) spin polarization at the Fermi energy as function of the chemical potential in the graphene layer and the spin down band center. The center of the spin up band is located in the optimal conductivity position, $\varepsilon_{0,\uparrow}=t$. We take $t_L=t_R=t_L'=t_R'$. The length of the graphene slab is set to $L=20\sqrt{3}a$. For larger values of L, the results are essentially identical.

sublattices.[43] We note that this result does depend on the fact that in our chosen geometry, zigzag edges present themselves to the leads, so that all the graphene sites contacting the leads are on the same sublattice. The sensitivity of the electronic states to the edge geometry is a well-known property of graphene.[44–46]

Finally, we analyze the magnetoresistance for *doped* graphene in the three stripe geometry. In this case the transport through the graphene part of the device is ballistic in the usual sense, and the MR has to be calculated as the relative change in the conductance, Eq. (13). In Fig. 7(a), we plot the MR for this case as a function of the chemical potential in the graphene and of the center of the spin down band. In addition, we plot the spin polarization at the leads. As in the case of undoped graphene, the MR is small (although not quite so small as in the undoped case), and only moderate values of MR result from large shifts between the centers of the spin up and spin down bands. From comparing the two panels of Fig. 7, we again observe that the values of MR and the spin polarization at the leads are largely uncorrelated.

IV. MAGNETORESISTANCE: FERROMAGNETIC TRANSITION METAL LEADS

Energy bands for ferromagnetic transition metals can be described approximately by using two bands, a d band characterized by a width $4t_d$ and center position ε_d and an s band with width $4t_s$ and center at ε_s.[47] Because of the shape of the atomic orbitals, the s band is much wider that the d band. Cobalt, for example, is a transition metal with a minority spin d band shifted up in energy relative to a majority spin d band. The s band is nearly spin unpolarized, and the Fermi energy crosses both the majority spin d band and the unpolarized s band, as illustrated in Fig. 1(b). For studying the transport properties of such systems, it is a good approximation to neglect the minority spin d band located at high energy.

We wish to consider the same device as studied in Sec. III with leads characterized by band structures of this sort. This can be modeled by assigning two orbitals to each site in the leads, one for the s band and the other for the d band. We can then assign on-site energies $\varepsilon_{s,d}$, respectively, for the two orbitals and hopping matrix elements t_s and t_d. These orbitals then connect to the p_z carbon graphene orbitals through hopping amplitudes t_s' and t_d', respectively. Although cobalt is a three dimensional metal, for simplicity, we treat it here as two dimensional. The resulting one-dimensional problem that one needs to treat for each k_y is illustrated in Fig. 2(c). Finally, for this section, we will restrict our discussion to the case of intrinsic graphene, $\mu=0$.

A. Conductivities

As there are two band orbitals in the transition metal leads, in order to compute the conductivity with different spin polarization orientations in the leads, we will need to evaluate several partial conductivities, representing transmission between different combinations of orbitals. These are the following.

(1) First is the conductivity across a graphene strip attached to single band spin-polarized metals, with the bands in the two leads centered at the same energies and having equal bandwidths,

$$\sigma_{\nu,\nu} = \frac{L}{W}\frac{1}{g_s}G(k_\nu), \tag{15}$$

where $G(k_\nu)$ is the conductance [Eq. (10)] evaluated with $k_L = k_R = k_\nu = \arccos\left(\frac{t_\nu - \varepsilon_\nu}{2t_\nu}\right)$. This contribution enters when we consider the transmission of spin-minority electrons in the parallel configuration, so that the d bands of the minority spin are high in energy in both leads and are irrelevant. Thus, only the band index $\nu = s$ for this contribution will be relevant in our calculation.

(2) Second is the conductivity of the device where the source and drain metals consist of two conducting bands, s and d. In this case, the conductivity per spin channel is

$$\sigma_{sd,sd} = \frac{e^2}{h}\frac{4g_v}{\pi}(t_s \sin k_s + t_d \sin k_d)^2 \frac{\arctan\left(\frac{\sqrt{4|a|^4 - (a^2 + a^{*2})^2}}{2|a|^2 - a^2 - a^{*2}}\right)}{\sqrt{4|a|^4 - (a^2 + a^{*2})^2}}, \tag{16}$$

with

$$a = t_s e^{ik_s} + t_d e^{ik_d}. \tag{17}$$

This contribution enters for spin-majority electrons when the lead polarizations are parallel.

(3) Finally, it is necessary to evaluate the conductivity in the case where the only available band in the source metal is the s band, whereas both bands, s and d, are available in the drain lead, or vice versa. These two situations arise when the lead polarizations are antiparallel. The required conductivities are both

$$\sigma_{s,sd} = \sigma_{sd,s} = \frac{e^2}{h}\frac{4g_v}{\pi}(t_s^2 \sin^2 k_s + t_s t_d \sin k_d \sin k_s) \frac{\arctan\left(\frac{\sqrt{4|b|^4 - (b^2 + b^{*2})^2}}{2|b|^2 - b^2 - b^{*2}}\right)}{\sqrt{4|b|^4 - (b^2 + b^{*2})^2}}, \tag{18}$$

with

$$b = (t_s e^{ik_s} + t_d e^{ik_d})e^{ik_s} t_s. \tag{19}$$

The above conductivities are independent of the values of the contact hopping amplitudes between the graphene orbitals and the s and d orbitals of the transition metal leads.

A very interesting result which emerges from Eqs. (15), (16), and (18) is that the conductivity of intrinsic graphene is nearly independent of the number of bands in the drain and source leads. For example, if we take $\varepsilon_s = t_s$ and $\varepsilon_d = t_d$, we find that all the conductivities are the same: $\sigma_{ss} = \sigma_{dd} = \sigma_{sd,s} = \sigma_{sd,sd} = (2/\pi)\frac{e^2}{h}$. (Note that we are evaluating the conductivity per spin channel.) Similarly, if we center all the bands at zero energy, $\varepsilon_s = \varepsilon_d = 0$, all the conductivities take the value $\sqrt{3}/4\frac{e^2}{h}$, independent of the hopping parameters. Figure 8 illustrates this behavior over a range of lead parameters. These results reflect the remarkably weak dependence of the graphene conductivity on the electronic structure of the contacts and, in particular, on the density of states of the metallic leads at the Fermi energy.

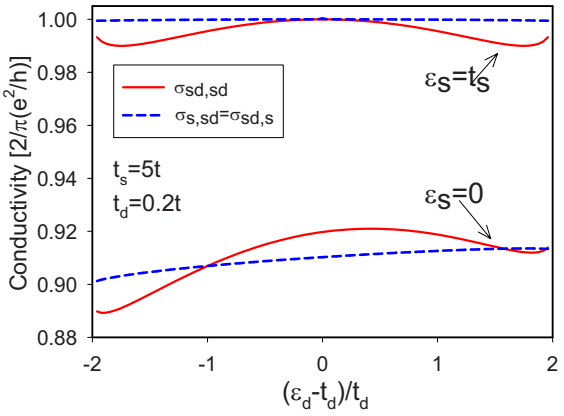

FIG. 8. (Color online) Conductivity per spin channel of a graphene slab connected to metallic leads with two (s and d) bands each, $\sigma_{sd,sd}$, and to a two orbital (s and d) source lead and a single orbital (s) drain lead, $\sigma_{sd,s}$. We plot the conductivity as a function of the band center of the d band. We assume that the s band is much wider than the d band, taking $t_s = 5t$ and $t_d = 0.2t$. Plotted are the $\varepsilon_\nu = t_\nu$ and the $\varepsilon_\nu = 0$ cases. Note that in all the cases, the conductivity depends weakly on the parameters of the metallic leads.

B. Magnetoresistance

For computing the magnetoresistance, we have to evaluate the conductivity in the parallel and antiparallel spin polarization configurations of the leads.

In the parallel configuration, majority spin electrons in the s and d bands of the metallic source are injected in the graphene slab and received in the majority spin s and d bands of the metallic drain. The minority spin electrons can go just from the source s band to the drain s band. Therefore, the conductivity is

$$\sigma_{para} = \sigma_{sd,sd} + \sigma_{s,s}. \tag{20}$$

In the antiparallel configuration, the majority spin electrons in the source can be in the s or d band. Upon passing through to the drain lead, these are now minority electrons, which can only reside in the s band. The inverse situation occurs for the minority spin carriers in the source lead. Thus, the conductivity in the antiparallel configuration takes the form

$$\sigma_{anti} = \sigma_{s,sd} + \sigma_{sd,s}. \tag{21}$$

Since by symmetry $\sigma_{s,sd} = \sigma_{sd,s}$, the magnetoresistance takes the form

$$\mathrm{MR} = \frac{\sigma_{sd,sd} + \sigma_{s,s} - 2\sigma_{s,sd}}{\sigma_{sd,sd} + \sigma_{s,s}}. \tag{22}$$

In Fig. 9(a), we plot our calculated magnetoresistance for this system. We assume the s band to be much wider than the d band and plot the results as functions of the energy center of the d band and for different positions of the center of the s band. In Fig. 9(b) we plot the corresponding spin polarization of the ferromagnetic leads. From Fig. 9, we immediately

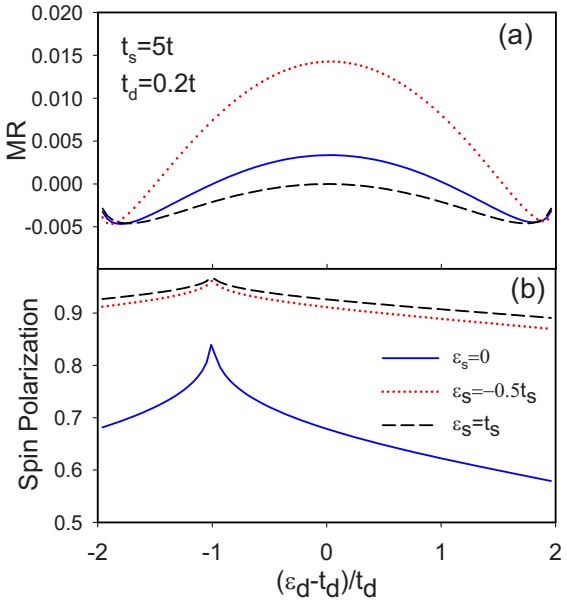

FIG. 9. (Color online) (a) Magnetoresistance of a graphene strip connected to ferromagnetic transition metal leads. (b) Spin polarization at the Fermi energy of the ferromagnetic leads. The *d* band is assumed to be much wider than the *s* band, $t_s=5t$ and $t_d=0.2t$, with *t* the graphene hopping parameter. We present the results for different positions of the center of the *s* band.

see that the magnetoresistance is generically very small, which we can again understand as a consequence of the relative insensitivity of the conductivity to the details of the leads. Interestingly, this same insensitivity means that there is no simple relationship between the value of the spin polarization in the leads and MR, as can be seen by comparing Figs. 9(a) and 9(b). (Note that the peak appearing in the polarization at $\varepsilon_d=0$ is due to a Van Hove singularity in density of states for a two dimensional square lattice in the tight-binding Hamiltonian.)

Finally, we note that recent experiments[35] on a graphene-based spin valve did lead to a significant MR for undoped graphene. Our results show that this result cannot be understood purely on the basis of a clean, noninteracting electron model. However, the ferromagnetic contacts reported by Hill *et al.* in Ref. 35 exhibited strongly non-Ohmic, nonlinear *I-V* behavior which one would not usually associate with normal metallic contacts.[48] When similar devices with Ohmic contacts (using a Ti sublayer) were fabricated, the magnetoresistance previously observed completely disappeared.[48] These experimental findings support our results that spin valves employing clean graphene and simple, homogeneously magnetized leads should have relatively very low MR.

V. SUMMARY AND CONCLUSION

In this work, we undertook a detailed study of the conduction properties of wide graphene strips, with two different models for the source and drain leads. We reconfirmed that for undoped graphene, the system can be described by a conductivity in the $L\to\infty$ limit even when defects are absent from the system and examined this behavior with respect to a broad range of lead parameters. The resulting conductance turns out to be relatively insensitive to these.

We then used these results to compute the magnetoresistance of a simple three stripe spin-valve device with graphene acting as the nonmagnetic material between the ferromagnetic leads. Two types of ferromagnetic lead systems were considered: one with a single (*s*) orbital for each spin state, with band centers separated in energy to induce spin polarization, and another with a narrow *d* band which was taken to be spin polarized. It was found that the MR was rather small for most circumstances in both cases, largely due to the insensitivity of the conductivity with respect to conditions in the leads.

ACKNOWLEDGMENTS

The authors thank J. J. Palacios, J. Fernández-Rosier, T. Stauber, B. Wunsch, E. Prada, and P. San-José for useful discussions. The authors are also grateful to André Geim for discussions about the results of Ref. 35. This work was supported by MAT2006-03741 (Spain) (L.B.), by the NSF through Grants Nos. DMR-0454699 and DMR-0704033 (H.A.F.).

[1] K. S. Novoselov, A. K. Geim, S. V. Mozorov, D. Jiang, Y. Zhang, S. V. Dubonos, I. V. Gregorieva, and A. A. Firsov, Science **306**, 666 (2004).
[2] K. S. Novoselov, A. K. Geim, S. V. Mozorov, D. Jiang, M. I. V. Gregorieva, S. V. Dubonos, and A. A. Firsov, Nature (London) **438**, 197 (2005).
[3] Y. Zhang, Y.-W. Tan, H. L. Stormer, and P. Kim, Nature (London) **438**, 201 (2005).
[4] Y.-W. Tan, Y. Zhang, K. Bolotin, Y. Zhao, S. Adam, E. Hwang, S. Das Sarma, H. L. Stormer, and P. Kim, arXiv:0707.1807 (unpublished).
[5] A. W. W. Ludwig, M. P. A. Fisher, R. Shankar, and G. Grinstein, Phys. Rev. B **50**, 7526 (1994).
[6] K. Ziegler, Phys. Rev. Lett. **80**, 3113 (1998).
[7] N. M. R. Peres, F. Guinea, and A. H. Castro-Neto, Phys. Rev. B **73**, 125411 (2006).
[8] M. I. Katsnelson, Eur. Phys. J. B **51**, 175 (2006).
[9] T. Stauber, N. M. R. Peres, and F. Guinea, arXiv:0707.3004 (unpublished).
[10] J. Martin, N. Akerman, G. Ulbricht, T. Lohmann, J. H. Smet, K. von Klitzing, and A. Yacoby, arXiv:0705.2180 (unpublished).
[11] V. Cheianov, V. Falko, B. Altshuler, and I. Aleiner, Phys. Rev. Lett. **99**, 176801 (2007).
[12] E. Hwang, S. Adam, and S. Das Sarma, Phys. Rev. Lett. **98**, 186806 (2007).
[13] J. C. Meyer, A. K. Geim, M. I. Katsnelson, K. S. Novoselov, T. J.

Booth, and S. Roth, Nature (London) **446**, 60 (2007).
[14] A. Castro Neto and E. A. Kim, arXiv:cond-mat/0702562 (unpublished).
[15] F. de Juan, A. Cortijo, and M. A. H. Vozmediano, Phys. Rev. B **76**, 165409 (2007).
[16] F. Guinea, M. I. Katsnelson, and M. A. H. Vozmediano, arXiv:0707.0682 (unpublished).
[17] L. Brey and J. J. Palacios, arXiv:0707.2358 (unpublished).
[18] J. Tworzydlo, B. Trauzettel, M. Titov, A. Rycerz, and C. W. J. Beenakker, Phys. Rev. Lett. **96**, 246802 (2006).
[19] E. Louis, J. A. Vergés, F. Guinea, and G. Chiappe, Phys. Rev. B **75**, 085440 (2007).
[20] H. Schomerus, Phys. Rev. B **76**, 045433 (2007); J. P. Robinson and H. Schomerus, *ibid.* **76**, 115430 (2007).
[21] Y. Blanter and I. Martin, Phys. Rev. B **76**, 155433 (2007).
[22] F. Miao, S. Wijeratne, Y. Zhang, U. C. Coskun, W. Bao, and C. N. Lau, Science **317**, 1530 (2007).
[23] K. Nomura and A. H. MacDonald, Phys. Rev. Lett. **98**, 076602 (2007).
[24] Z. Chen, Y.-M. Lin, M. J. Rooks, and P. Avouris, arXiv:cond-mat/0701599 (unpublished).
[25] M. Y. Han, B. Ozyilmaz, Y. Zhang, and P. Kim, Phys. Rev. Lett. **98**, 206805 (2007).
[26] D. Huertas-Hernando, F. Guinea, and A. Brataas, Phys. Rev. B **74**, 155426 (2006).
[27] I. Zutic, J. Fabian, and S. Das Sarma, Rev. Mod. Phys. **76**, 323 (2004).
[28] B. Trauzettel, D. V. Bulaev, D. Loss, and G. Burkard, Nat. Phys. **3**, 192 (2007).
[29] Y. G. Semenov, K. W. Kim, and J. M. Zavada, Appl. Phys. Lett. **91**, 153105 (2007).
[30] H. Haugen, D. Huertas-Hernando, and A. Brataas, arXiv:0707.3976 (unpublished).
[31] V. M. Karpan, G. Giovannetti, P. A. Khomyakov, M. Talanana, A. A. Starikov, M. Zwierzycki, J. van den Brink, G. Brocks, and P. J. Kelly, Phys. Rev. Lett. **99**, 176602 (2007).
[32] N. Tombros, C. Jozsa, M. Popinciuc, H. T. Jonkman, and B. J. van Wees, Nature (London) **448**, 571 (2007).
[33] S. Cho, Y.-F. Chen, and M. S. Fuhrer, Appl. Phys. Lett. **91**, 123105 (2007).
[34] M. Ohishi, M. Shiraishi, R. Nouchi, T. Nozaki, T. Shinjo, and Y. Suzuki, Jpn. J. Appl. Phys., Part 2 **46**, L605 (2007).
[35] E. Hill, A. K. Geim, K. Novoselov, F. Schedin, and P. Blake, IEEE Trans. Magn. **42**, 2694 (2006).
[36] E. Louis, J. A. Vergés, F. Guinea, and G. Chiappe, J. Phys. F: Met. Phys. **6**, 849 (1976).
[37] S. Datta, *Electronic Transport in Mesoscopic Systems* (Cambridge University Press, Cambridge, 1997).
[38] F. Munoz-Rojas, J. Fernandez-Rossier, L. Brey, and J. J. Palacios, arXiv:0707.0375 (unpublished).
[39] E. N. Economou, *Green's Functions in Quantum Physics* (Springer-Verlag, Berlin, 1983).
[40] M. Julliere, Phys. Lett. **54A**, 225 (1975).
[41] L. Brey, C. Tejedor, and J. Fernández-Rossier, Appl. Phys. Lett. **85**, 1996 (2004).
[42] G. Schmidt, D. Ferrand, L. W. Molenkamp, A. T. Filip, and B. J. van Wees, Phys. Rev. B **62**, R4790 (2000).
[43] L. Brey, H. A. Fertig, and S. Das Sarma, Phys. Rev. Lett. **99**, 116802 (2007).
[44] K. Nakada, M. Fujita, G. Dresselhaus, and M. S. Dresselhaus, Phys. Rev. B **54**, 17954 (1996).
[45] L. Brey and H. A. Fertig, Phys. Rev. B **73**, 235411 (2006).
[46] L. Brey and H. A. Fertig, Phys. Rev. B **73**, 195408 (2006).
[47] W. A. Harrison, *Electronic Structure and the Properties of Solids* (Dover, New York, 1980).
[48] A. Geim (private communication).